Journal of Applied Electrochemistry **31**: 387–394, 2001.

Electrochemistry of the SUCOPLATE® electroplating bath for the deposition of a Cu–Zn–Sn alloy
Part I: Commercial bath

L. PICINCU[1], D. PLETCHER[1]* and A. SMITH[2]
[1]*Department of Chemistry, The University, Southampton, Southampton SO17 1BJ, UK*
[2]*Huber & Suhner (UK) Ltd, Telford Road, Bicester, Oxfordshire OX6 0LA, UK*
*(*author for correspondence, e-mail: dp1@soton.ac.uk)*

Received 8 May 2000; accepted in revised form 24 October 2000

Key words: alloy deposition, bath components, Cu–Zn–Sn, electroplating

Abstract

The deposition of a Cu–Zn–Sn alloy from a commercial alkaline cyanide electroplating bath operated at 333 K has been investigated using voltammetric techniques and electron microscopy. It is shown that a highly reflecting alloy deposit with a composition in the range 47–51% copper, 8–12% zinc and 38–43% tin can be produced under a range of conditions. In addition, it is concluded that the rate of alloy deposition is partially limited by mass transport and partially by the kinetics of reactions in homogeneous solution.

1. Introduction

The electroplating of alloys is an established part of the metal finishing industry and typical baths have been described in a number of books [1–5]. The influence of the plating conditions (e.g., bath composition, current density, temperature) on the composition of the electroplated alloy and the properties of the deposit are, however, far from well understood. Huber & Suhner Ltd employ an alkaline cyanide plating bath (tradename SUCOPLATE®) operated at 333 K for the electrodeposition of a bright, abrasion resistant Cu–Zn–Sn alloy for finishing electronic components [6]. This plating bath clearly falls into the classification of a highly complexed, high throwing power solution but the bath composition is not similar to those reported earlier for other Cu–Zn–Sn alloys and leads to alloys with a quite different composition [3]. This paper therefore reports the electrochemistry of the SUCOPLATE® plating bath and describes the morphology and composition of the deposit formed in common operating conditions. The influence of the concentration of bath components on the electrochemistry of the system, alloy composition and deposit quality is examined and described in Part II of this paper [7].

2. Experimental details

All experiments were carried out with fresh solutions prepared with water from a Whatman Still Plus and RO50 system and high quality chemicals supplied by Huber & Suhner (UK) Ltd. The solution composition used throughout this paper is stated in Table 1. Copper Glo solution is an electroplating additive supplied by LeaRonal Ltd where the active ingredient is believed to be an aliphatic tertiary amine oxide with a long chain amide substituent. The free (uncomplexed) cyanide and free hydroxide concentrations were adjusted after the preparation of all solutions and these concentrations were determined using a Metrohm Titroprocessor 686 with prescribed procedures. The solution was thermostatted, usually at a temperature of 333 K, and consistent with commercial practice, was not deoxygenated. The substrate for electroplating was either brass (68% Cu, 32% Zn) or the brass covered with a silver strike. In Hull cell experiments, the substrates were 100 mm × 75 mm brass plates supplied by Ossian Ltd; these were prepolished and supplied with a protective film on the face to be plated. Before use, they were electrocleaned (1 A for 60 s) in an alkaline bath at 313 K and then acid etched. In other experiments, the working electrode was a strip, 5 mm wide, cut from a brass plate and mounted so that it dipped into the solution to a depth of 10 mm; these make convenient disposable electrodes with an active area of 1 cm^2.

Two cells were used. Voltammetry and other experiments with the strip electrodes were carried out in a glass cell with a water jacket and a capacity of ~20 cm^3. The strip working electrode (area ~ 1 cm^2) and Pt gauze counter electrode were in the same compartment while the saturated calomel (SCE) reference electrode was

Table 1. Composition of the electroplating bath used for all experiments in this paper

Bath component	Concentration	
	/g l^{-1}	/mM
CuCN	9.1	102
$Zn(CN)_2$	5.4	46
$Na_2Sn(OH)_6$	5.7	24
Na_2CO_3	6.5	61
Free NaCN	25.0	551
Free NaOH	2.1	50
Copper Glo solution	5.0	–

separated from the working electrode by a Luggin capillary. The Hull cell was undivided, fabricated from Perspex and had a capacity of ~300 cm^2. The separation of the brass plate (dimensions 100 mm × 75 mm) and the steel counter electrode ranged from 45 to 125 mm. The solution was agitated slowly with a paddle stirer which moved across the surface of the brass plate.

The voltammetric experiments were carried out using an EG&G PAR Model 263 Electrochemical System. The data acquisition was performed using an Opus 386 computer via a GPIG-PC 2A (National Instruments) using the EG&G software package M270, version 4.23. The data were then imported into a Dell Pentium 75 computer for further analysis using the same software. The electrodeposition experiments were controlled with a Powerline 30 V, 2.5 A power supply. Scanning electron microscopy was carried out using a Jeol, model JSM 6400 microscope with an accelerating voltage of 20 kV and equipped with a Tracor series II X-ray and image analysis system for energy dispersive analysis (EDX).

3. Results

3.1. *Cyclic voltammetry*

Figure 1 shows cyclic voltammograms recorded with a potential scan rate of 20 mV s^{-1} at a brass strip electrode in the plating bath at 333 K. The positive limits are −1260 mV vs SCE, a potential where the current is zero and no alloy was deposited; corrosion of the brass commences at potentials just positive to this value. The negative potential limit is −2000 mV where H_2 evolution is clearly observed; beyond −2000 mV, the current rises steeply and smoothly to very large values. Figure 1(a) shows the first scan on the brass electrode. The main feature is a cathodic peak, $E_p = -1680$ mV vs SCE and $I_p = 5.2$ mA cm^{-2}. This peak current density is a large fraction of the current density commonly used in commercial plating (6 mA cm^{-2} is a typical value) but significantly less than would be estimated for a diffusion controlled reduction of all the Cu(I), Zn(II) and Sn(IV) in solution. When compared with the peak shape expected for a diffusion controlled process, however, this cathodic peak is too symmetrical, the current dropping too rapidly beyond the peak. In addition, H_2 gas could be seen to evolve from the electrode while the potential is scanned through the region of the peak; the rate of bubble formation then decreased again at more negative potentials before becoming increasingly vigorous beyond −2000 mV. Hence, it was concluded that H_2 evolution is a major contributor to the current in the potential range around this peak but becomes inhibited at more negative potentials. The inhibition of H_2 evolution could result from a change to the electrode surface, either the composition of the deposit or the adsorption of an organic species (the additive or a compound derived from the additive) or hydrogen atoms adsorbing on the freshly deposited alloy surface in this potential range. In other experiments, it was shown that the peaked response in the voltammogram and H_2 evolution around −1600 mV are only observed when the organic additive is present in solution. Therefore, Copper Glo is certainly implicated in the electrode reactions in this potential region.

After a single potential cycle, the brass is obviously covered with a uniform, shiny and silver coloured alloy layer and, indeed, the total cathodic charge passed (~130 mC cm^{-2}) is sufficient to deposit a layer ~ 0.2 μm

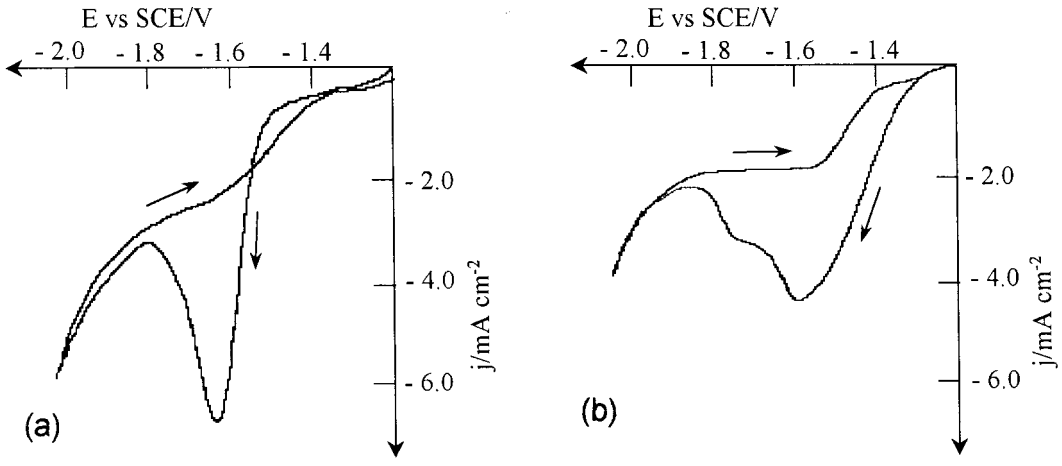

Fig. 1. Cyclic voltammograms for the electroplating bath at a fresh brass strip electrode (a) first scan (b) fourth scan after continuous potential cycling. Potential scan rate 20 mV s^{-1}. Temperature 333 K.

thick if metal deposition were the only electrode reaction taking place (in reality, as described above, H_2 evolution is a significant contributor to this cathodic charge). In fact, alloy can be seen to be deposited on the brass even if the negative limit for the potential cycle is −1600 mV or the potential is held negative to −1500 mV for a short period and there can be no doubt that the cathodic peak in the voltammogram signals the deposition of alloy in addition to the contribution to the current due to H_2 evolution. The reverse scan in Figure 1(a) shows no anodic current negative to −1300 mV; the reduction is irreversible and the Cu–Zn–Sn alloy appears to be stable to corrosion over the potential range studied. The reverse scan also shows a narrow potential range around −1520 mV where the current is higher than on the forward scan and this is consistent with the process leading to the cathodic peak on the forward scan involving a nucleation step for the formation of a new phase on the electrode surface. Figure 1(b) reports the current/potential response during the fourth continuous potential cycle and there are significant differences. Although the cathodic peak remains at a similar potential, it is smaller with a peak current density of ~ 4 mA cm^{-2}. It is also much broader because reduction starts much earlier at −1380 mV (cf. −1520 mV on the first cycle). The fourth scan also shows a new shoulder at −1760 mV. If there is a pause of 100 s with agitation between the 3rd and 4th scan, the positive shift in the foot of the first cathodic peak and the shoulder at −1760 mV are still seen although the currents are larger than without the pause. The changes between the 1st and 4th cycles therefore result from the different surface properties of brass and the Cu–Zn–Sn alloy (not changes to the solution adjacent to the electrode). It is tempting to interpret the positive shift in the reduction potential only in terms of a higher rate of metal deposition on the Cu–Zn–Sn alloy surface (4th cycle) than on brass (1st cycle). In fact, however, H_2 evolution is also observed around −1500 mV on the 4th scan but not the 1st and this reaction is again contributing to the current observed.

In cyclic voltammetry, the extent of diffusion control is usually probed by variation of the potential scan rate. Such experiments, however, gave complex results and experiments at faster scan rates led to peaks whose shape imply a role for adsorption processes. Therefore, the importance of mass transport in determining the magnitude of the current densities was examined using a rotating disc electrode. Figure 2 shows voltammograms recorded at a rotating brass disc electrode, rotation rates 400 rpm and 3600 rpm. A reduction 'wave', $E_{1/2} \approx$ −1660 mV vs SCE can be discerned but the voltammograms do not have a classical shape and well formed plateaux are not observed. Rather, negative to the wave, the current shows some decrease consistent with passivation. It should, however, be noted that the currents are significantly higher at the faster rotation rate but not by the factor of three predicted by the Levich equation for a mass transfer controlled current. Moreover, the

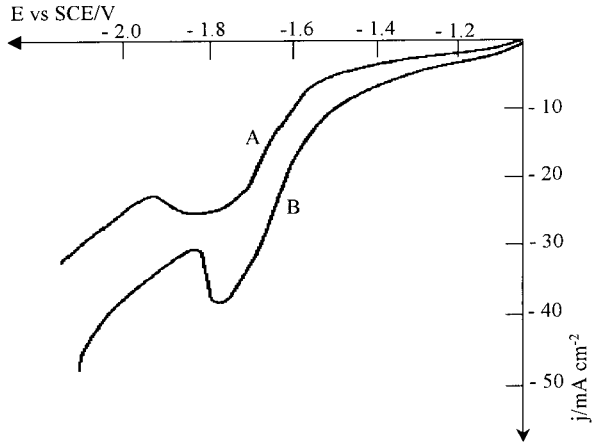

Fig. 2. Voltammograms for the electroplating bath at a polished brass rotating disc electrode. Rotation rate (a) 400 rpm (b) 3600 rpm. Potential scan rate 20 mV s^{-1}. Temperature 333 K.

limiting current density at 400 rpm is 28 mA cm^{-2} compared to a value of 160 mA cm^{-2} estimated from the Levich equation for mass transport control with respect to all the Cu(I), Zn(II) and Sn(IV) in the bath (assuming a diffusion coefficient of 6×10^{-6} cm^2 s^{-1} for each metal species in solution). In the potential region negative to the 'wave', the rate of alloy deposition therefore appears to be partially mass transport limited but with quite significant control by some chemical processes in solution, probably changes to the speciation of the metal ions before electron transfer. Further evidence in support of this conclusion results from voltammetry carried out as a function of temperature. At 293 K, voltammograms shows no waves or peaks positive to −1800 mV and the characteristic response described above develops as the temperature is increased. The current densities observed at −1700 mV vs SCE. during a linear potential scan at 20 mV s^{-1} are reported in Table 2. The very strong dependence of the rate of alloy deposition on temperature is clearly seen and this implies that the rate is determined largely by a chemical step.

3.2. *Steady state experiments*

A series of experiments was carried out, each using a fresh brass strip electrode in unstirred solution. The potential of the brass strip electrode was held constant at a value in the range from −1500 mV to −2200 mV vs

Table 2. Currents measured at −1700 mV vs SCE from linear potential sweep experiments at 20 mV s^{-1} as a function of temperature

Temperature/K	j/mA cm^{-2}
293	0.8
313	1.2
333	5.2
343	9.5

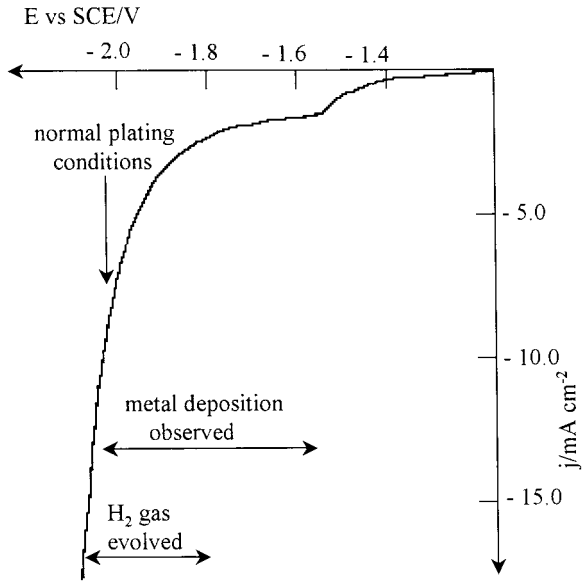

Fig. 3. Steady state voltammogram recorded for the electroplating bath at a fresh brass strip electrode after it had been held at −2200 mV vs SCE for 60 s. Potential scan rate 20 mV s^{-1}. Temperature 333 K.

SCE until the current reached a constant value (typically after 50–500 s) and then the potential was scanned in the positive direction. Figure 3 shows a typical voltammogram, in fact that recorded after the potential had been held at −2200 mV for 60 s. The voltammogram again shows a reduction wave at −1650 mV with a limiting current density of ~ 2 mA cm^{-2}. Negative to −1800 mV the cathodic current rises steeply. Observation of gas evolution and alloy deposition allows the source of these currents to be identified, see Table 3:

(i) Alloy was deposited at all potentials negative to −1500 mV vs SCE. The deposits showed strong adhesion and were both reflecting and uniform. Hence, the reduction wave is associated with metal deposition although the limiting current is low compared to the commercial plating current density of 6 mA cm^{-2}.

(ii) At the bath pH of 13.2, the equilibrium potential for H_2 evolution is about −1100 mV and, hence, H_2 evolution is thermodynamically favourable over all the potential range studied. In practice, continuous hydrogen evolution was always visible at potential negative to −1900 mV and becomes increasingly vigorous as the potential is made more negative. By −2200 mV it is the dominant cathodic reaction and leads to the increase in current in this potential range. It should be emphasized that H_2 evolution was observed early in depositions at around −1600 mV but only as a transient phenomenon. A burst of gas bubbles was seen for several seconds and then dies away.

The current density often used in commercial plating, 6 mA cm^{-2}, corresponds to a potential of −2050 mV vs SCE. This was also confirmed by chronopotentiometry, see Figure 4. When a current density of 6 mA cm^{-2} is applied, the potential changes rapidly from the open circuit value to −1760 mV but within 2 s, reaches a steady state value of −2050 mV vs SCE. The Figure also shows the responses at other current densities; the results are entirely consistent with the voltammetry. With current densities in the range 4–10 mA cm^{-2}, the E/t curves all show evidence for an electrode reaction around −1700 mV before the potential moves to a steady state value in the H_2 evolution region. The response at 2 mA cm^{-2} is different. The steady state potential is −1550 mV and the steady state is reached via an excursion to more negative potentials. This is typical of an electrode reaction where phase formation is occurring and the rate of nucleation of the new phase on the electrode surface influences the response. At higher current densities nucleation becomes too fast to see this excursion.

3.3. *Chronamperometry*

The nucleation and early growth of a metal layer is better studied by potential step experiments and Figure 5 reports I/t transients for a series of potential steps from −1250 mV to values in the range −1320 mV to −1400 mV. It can be seen that, at these potentials well positive to the wave in the steady state voltammogram,

Table 3. Steady state currents and visual observation during potentiostatic experiments

Potential /mV vs SCE	Current density /mA cm^{-2}	Alloy deposition	H_2 evolution
−1400	−0.4	None observed after 600 s	None visible
−1500	−0.8	None observed after 600 s	None visible
−1600	−1.4	Tarnished with bronze tinge	Transient
−1700	−2.3	Highly reflecting	Slight
−1800	−2.6	Highly reflecting	Slight
−1900	−3.5	Highly reflecting	Slight
−2000	−5.5	Highly reflecting	Vigorous
−2100	−7.0	Highly reflecting	Vigorous
−2200	−20	Highly reflecting	Vigorous

Temperature 333 K

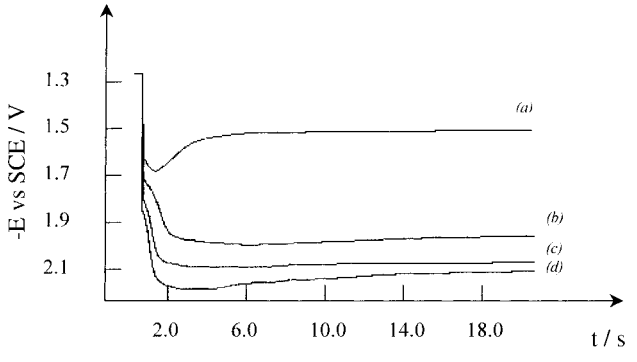

Fig. 4. Chronopotentiometry for a fresh brass strip electrode in the electroplating bath. Current densities (a) 2, (b) 4, (c) 6 and (d) 10 mA cm^{-2} . Temperature 333 K.

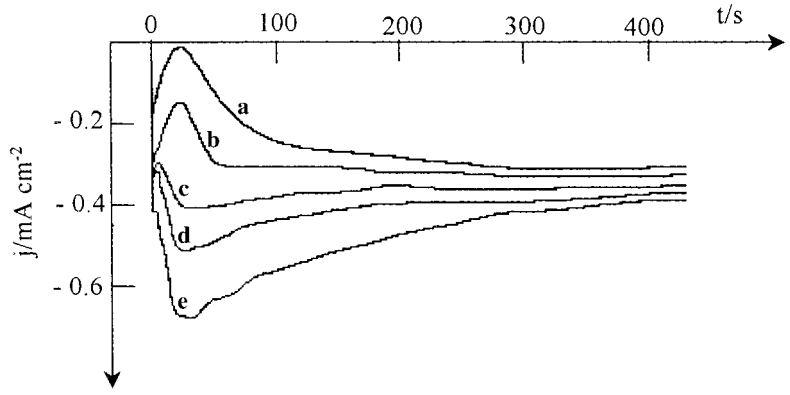

Fig. 5. Current–time transients in response to potential step experiments from −1250 mV to (a) −1320, (b) −1340, (c) −1360, (d) −1380 and (e) −1400 mV vs SCE. Fresh brass strip electrodes in the electroplating bath at 333 K.

alloy deposition is occurring, albeit at a very low rate. At each potential, an early fall in current is followed by a rising cathodic current over a timescale of 50–150 s and eventually a steady state current is reached. As the potential is made more negative, the timescale for the rise in current becomes shorter and there is a trend for the transient to pass through a maximum before decaying towards a steady state current that increases as the potential is made more negative. If the potential is stepped to −1700 mV, only a falling I/t transient is observed and the steady state current is about 2.2 mA cm^{-2}, close to that observed by steady state voltammetry. The early parts of the rising portions of the transients observed in the potential range, −1320 mV to −1400 mV, could be fitted to linear $I^{1/3}$ against t plots as expected for continuous nucleation and three dimensional growth of centres under electron transfer control. Certainly, the overall picture is consistent with a mechanism for alloy deposition where nucleation of the Cu–Zn–Sn alloy phase on the brass surface is followed by three dimensional growth of the nuclei and overlap of the centres into a continuous layer. This layer then thickens under partial mass transfer and partial kinetic control. The influence of nucleation is, however, only evident at low overpotentials and it is clear that in the conditions of commercial plating, nucleation is very rapid.

3.4. *Scanning electron microscopy*

A large number of scanning electron micrographs were obtained during this programme. Many samples were prepared in the laboratory and others were taken from the commercial plating lines (both jig and barrel plating). Energy dispersive spectroscopy (EDX) was used for routine elemental analysis of the plated layers. In order to ensure that the determination of the elemental composition was not influenced by penetration of the electron beam into the brass substrate, it was found essential either to use deposits which were relatively thick or to undercoat the samples with a silver strike (as is, anyway, common in commercial practice). For example, in a common Hull cell test where plating was carried out at 1 A for 120 s, the deposit at the position for 6 mA cm^{-2} appeared good but was not thick enough to obtain reliable compositional data by EDX; the % Cu and % Zn were always high due to the electron beam entering the brass substrate.

Figure 6(a) is an SEM of a sample cut from an uncoated Hull cell brass plate. It can be seen that the surface is covered by an array of scratches resulting from the polishing procedure. Figure 6(b) shows an SEM of a brass strip electrode which has been plated at a constant potential of −2050 mV for 120 s and it can be seen that the surface of the plate is significantly smoother although there are a few linear features which may result from the existence of scratches on the brass substrate. Rather featureless surfaces were also obtained by plating at 6 mA cm^{-2} for 120 s whether on a strip electrode, a Hull cell plate or, indeed, on commercial samples. Also, undercoating with a silver strike did not change the morphology of the surface after alloy plating. Commonly, on the commercial plating line, deposition is continued over a longer period in order to give a thicker deposit. Figure 6(c) shows the SEM of a surface after plating at 6 mA cm^{-2} for 900 s and some rounded features are beginning to be observed. By eye, this deposit looks as reflecting as the thinner deposits obtained in the laboratory.

The elemental composition for a number of samples plated under different conditions in the laboratory, as well as a sample from the commercial line, are reported in Table 4. With the exception of the thick deposit, the elemental compositions are very similar and this was confirmed with many other samples. It was concluded that the composition of highly reflecting and fault free deposits lay in the ranges: Cu 47–51%, Zn 8–12% and Sn 38–43%. This alloy composition is quite different from the molar ratio of the metal ions in solution (Cu:Zn:Sn = 60:28:12). This is not possible if the deposition is mass transport controlled and the alloy composition must be determined by kinetic factors. Clearly, the kinetics of tin deposition must be favourable compared particularly to zinc. A series of depositions were also carried out as a function of temperature (293–343 K); while the rate of deposition obviously increased

with increase in temperature, the composition always fell in the normal range, see above.

A Hull cell deposition is generally used for quality control of this alloy plating bath. It has been found that a particular appearance of the whole plate after deposition of alloy at 1 A for 120 s correlates well with a healthy bath with an acceptable composition. The test leads to a plate where most of the surface appears uniformly coated with highly reflecting, silver coloured alloy but at the high current density side there is an area which is darker and striped in appearance (known as 'tiger stripe'). Low resolution SEM show that the striped appearance is due to ridges of thick deposit with thinner deposit between. Figure 7(a) illustrates an SEM of the thicker deposit in the tiger stripe region on a Hull cell plate and it can be seen that the deposit is now made up of many overlapping small hemispherical centres. The regions between the 'ridges' have a similar morphology and alloy composition. Table 5 reports the compositions for deposits on different areas of a silver undercoated Hull cell plate. It can be seen that with increasing current density, the % Cu increases at the expense of tin in the electroplate and the deposit darkening can be associated with high copper. Another phenomenon was observed when the bath required adjustment to its composition. In the low current density region of the plate, tarnishing by a diffuse white film was seen. EDX analysis of such areas showed them to be rich in tin and SEM reveals a surface made up of many overlapping, small and angular crystallites, see Figure 7(b).

In a further series of experiments, deposition was carried out onto silver undercoated strip electrodes at a series of potentials. At each potential, deposition was continued until a charge of 0.8 C cm^{-2} had been passed. The compositions are shown in Table 6. At −1500 mV,

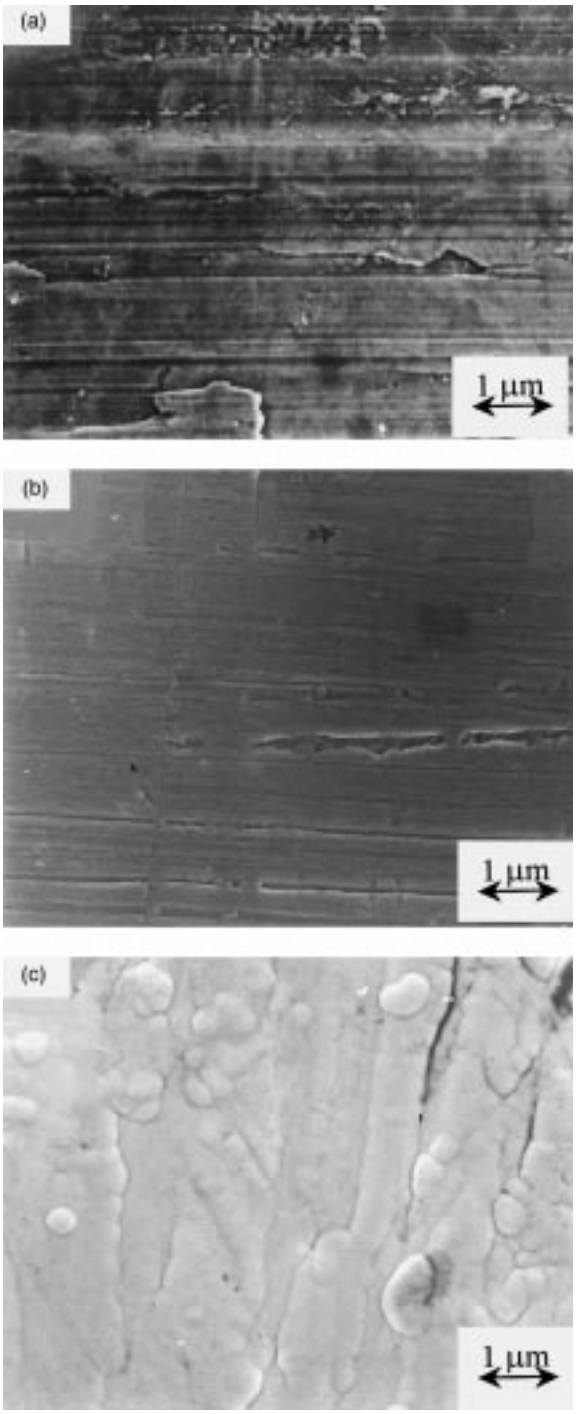

Fig. 6. Scanning electron micrographs of (a) the brass substrate and (b) the surface after the deposition at −2050 mV for 120 s, (c) the surface after the deposition at 6 mA cm^{-2} for 900 s Temperature 333 K.

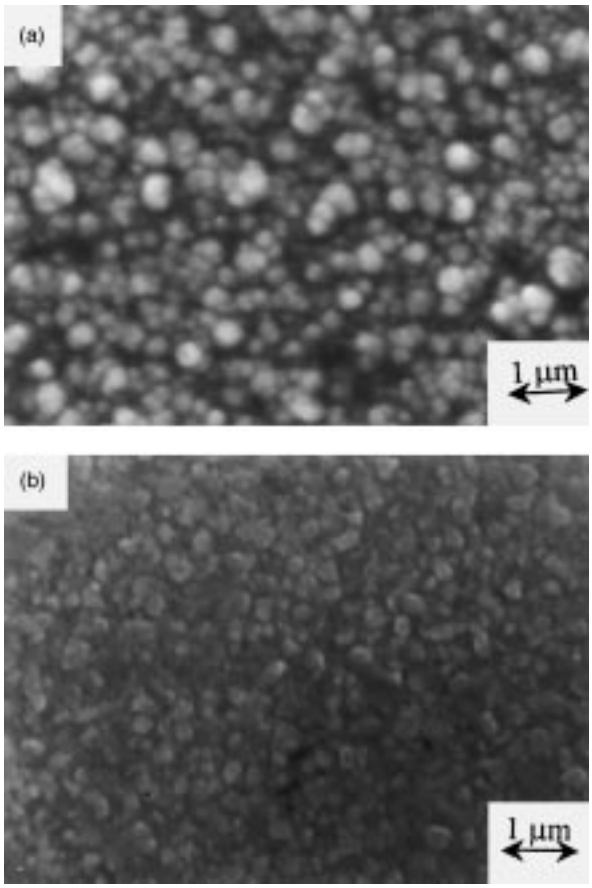

Fig. 7. Scanning electron micrographs of the Cu–Zn–Sn alloy deposit from a Hull cell (a) at the position for a current density of 40 mA cm^{-2}, (b) at a current density of 6 mA cm^{-2} when there is tarnishing of the deposit. Deposition time 120 s. Temperature 333 K.

Table 4. Composition of substrate and alloy deposits determined by EDX analysis

Electroplating conditions	Elemental composition/%		
	Cu	Zn	Sn
Brass substrate	68	32	
Ag plated brass strip, $I = 6$ mA cm^{-2}	50	9	41
Ag plated brass strip, $E = -2050$ mV	50	9	41
Hull cell, Ag plated plate at position for $I = 6$ mA cm^{-2}	51	8	41
Hull cell brass plate, thick alloy deposit† at position for $I = 6$ mA cm^{-2}	54	8	36
Plated component from commercial line†	48	8	43

Laboratory depositions at 333 K using a total charge of about 1 C cm^{-2} except † about 10 C cm^{-2}

Table 5. EDX analysis of a sample from Hull cell deposit on a Ag coated brass plate

Hull Cell Plate	Sample	I/mA cm^{-2}	Cu/%	Zn/%	Sn/%
C B A	A	6	50	10	40
	B	13	53	10	37
	C	45	57	12	31

Temperature 333 K

the deposit is reddish brown and the alloy has a high copper content at the expense of both tin and zinc; this might be expected if Cu(I) is easier to reduce than the other two ions. Negative to the wave in the steady state voltammogram, the composition becomes independent of the applied potential and close to those reported in Table 4.

The experiments reported in this paper all used freshly prepared solutions. In a plating line, however, the bath may be in use for many weeks. Since there is the possibility that the metal ion speciation changes with time, the influence of lifetime of the solution was checked. A standard solution was investigated immediately after preparation and then after 1 day and 2 weeks; in each case the free cyanide and free hydroxide concentrations were checked and, if necessary, adjusted back to their specified levels. The cyclic voltammograms for the three solutions were identical. Moreover, electroplates on to Ag undercoated strip substrates from the fresh and aged solutions were all uniform and highly reflecting and the alloy compositions were Cu 50 ± 1%, Zn 8 ± 1%, Sn 42 ± 1%. Although the performance of the plating bath changes with use within a plating line (although concentrations are regularly adjusted), that of the bath solution does not appear to change on standing without passage of charge.

Table 6. Composition of the alloy electroplated as a function of deposition potential

Potential /mV	Current density /mA cm^{-2}	Elemental composition/%		
		Cu	Zn	Sn
−1500	1.0	67	2	31
−1600	2.3	58	6	36
−1700	2.3	53	9	41
−1900	3.6	47	8	45
−2050	6	51	8	41

Charge passed 0.8 C cm^{-2}, Temperature 333 K

4. Discussion

It is shown that a Cu–Zn–Sn alloy layer may be plated onto brass or brass with a Ag strike under a range of controlled current or controlled potential conditions. The alloy is adherent and has a composition within a defined range. It also appears uniform and is highly reflecting and silver in colour. In the conditions typical of commercial electrodeposition, hydrogen evolution accompanies the metal ion reduction reactions and this will enhance local mass transport and may also improve the throwing power of the bath. Certainly, the electron micrographs of the electrodeposits under preferred conditions do not show any pronounced surface morphology. At very high current density, the deposit is rich in copper and low in tin and this leads to a darker striped deposit; electron microscopy shows that such deposits are made up of overlapping hemispheres with submicrometric radii. A copper rich deposit was also found at very low negative potentials (i.e., low current densities).

In steady state voltammetry, a single reduction wave at −1650 mV may be identified with the electrode reactions leading to alloy deposition. It was never possible to identify separate waves/peaks for the reduction of Cu(I), Zn(II) and Sn(IV) species and it must be concluded that there are cooperative effects in the mechanism of simultaneous deposition of the three metals; the kinetics of alloy deposition are quite different from those for each of the individual metals. The height of this wave and its dependence on rotation rate would indicate that the limiting current is partially controlled by mass transfer at a temperature of 333 K. On the other hand, the strong variation of the current density with the temperature and the composition of the alloy (i.e., quite different from the solution composition) clearly indicate rate control by homogeneous chemical reactions prior to electron transfer. It is likely that the speciation of the metal ions must change before reduction is possible. The mixed control for metal ion reduction will also determine the alloy deposition rate at the more negative potential consistent with commercial conditions.

Non-steady state experiments allow the investigation of the nucleation and early growth of the alloy phase on the cathode surface but nucleation is clearly a very rapid process in commercial conditions. They also disclose that the ratio of hydrogen evolution/metal deposition can change with time and the voltammograms contain peaks which would be consistent with passivation and adsorption processes involving the Copper Glo additive and/or hydrogen atoms.

The following paper will report experiments using electroplating baths with other compositions as well as investigations of the mode of action of the organic additive.

Acknowledgements

The authors would like to thank Huber & Suhner (UK) Ltd for financial support of this programme, the supply of equipment, chemicals and components as well as advice and encouragement.

References

1. A. Brenner, 'Electrodeposition of Alloys', Volumes I and II, Academic Press, New York, (1963).
2. F.A. Lowenheim (Ed), 'Modern Electroplating', Wiley Interscience, New York, (1974).
3. M. Jordan, 'The Electrodeposition of Tin and its Alloys', Eugen G. Leuze, Saulgau/Würtz, Germany, (1995).
4. 'Canning Handbook on Electroplating', 21st edn, W. Canning & Co, Birmingham, (1970).
5. D. Pletcher and F.C. Walsh, 'Industrial Electrochemistry', 2nd edn, Chapman & Hall, London, (1990).
6. Huber & Suhner Ltd, Technical Literature.
7. L. Picincu, D. Pletcher and A. Smith, *J. Appl. Electrochem.*, this issue.